We are IntechOpen, the world's leading publisher of Open Access books Built by scientists, for scientists

6,900
Open access books available

185,000
International authors and editors

200M
Downloads

154
Countries delivered to

Our authors are among the

TOP 1%
most cited scientists

12.2%
Contributors from top 500 universities

CLARIVATE ANALYTICS
BOOK CITATION INDEX
INDEXED

WEB OF SCIENCE™

Selection of our books indexed in the Book Citation Index
in Web of Science™ Core Collection (BKCI)

Interested in publishing with us?
Contact book.department@intechopen.com

Numbers displayed above are based on latest data collected.
For more information visit www.intechopen.com

Compensation of Frequency-Dependent Attenuation for Tissue Harmonic Pulse Compression Imaging

Norio Tagawa, Takuya Hiraoka and Iwaki Akiyama

Additional information is available at the end of the chapter

Abstract

Tissue harmonic imaging (THI) is highly effective for correct diagnosis. On the other hand, pulse compression is often used in a radar system and an ultrasound imaging system to perform high SNR measurement. Therefore, the performance of pulse compression of tissue harmonic imaging is required to be improved. The frequency-dependent attenuation (FDA) is a crucial problem in medical tissue imaging. In the pulse compression imaging, the deterioration of echoes by the FDA lowers the performance of a matched filtering using an ideal transmitted pulse as a template signal. Since, especially in the harmonic imaging, higher-frequency components are used for imaging than the fundamental imaging, the compensation of the FDA is strongly important for high-definition imaging. In this study, we examine a method to reduce the influence of the FDA on harmonics.

Keywords: FDA, pulse compression, tissue harmonic imaging, FM chirp, compensation for FDA

1. Introduction

The ultimate goal of our study is to perform high-resolution and high signal-to-noise ratio (SNR) ultrasound imaging required for high-quality diagnosis. Such imaging is strongly demanded particularly in the deep part of a living body. On the other hand, we are developing a puncture ultrasound microscope [1–3], in which echo is very weak and cell-level resolution is required, so high-definite imaging technique is absolutely important. A pulse compression technique (PCT) is effective for improving SNR while maintaining safety to the living body [4–6].

In PCTs, broadband modulation is necessary to improve the range resolution. The bandwidth that is used efficiently for transmission and reception is limited by the resonance characteristics of the transducer that utilizes thickness resonance vibration. In order to widen the bandwidth of the transducer, a layered-type transducer has been developed in which two piezoelectric oscillators having different thicknesses are longitudinally bonded and one of a pair of electrodes is inserted between two oscillators [7]. In addition, we are proposing the concept of a new transducer based on a PMUT structure with a thicker diaphragm than conventional PMUT and by which the bandwidth can be greatly widened [8]. In general, the wide bandwidth of the transmitted pulses is a prerequisite for sharp pulses. Therefore, broadband transmission in PCTs improves range resolution. On the other hand, in order to improve the SNR by PCTs, it is necessary to increase energy inflow into the body by transmitting a signal with a wide pulse width. Namely, a PCT using pulses having a wideband and a wide pulse width is suitable for our objective.

Due to its high resolution, tissue harmonic imaging (THI) is useful, and many studies have been done [9, 10]. THI uses harmonic components generated as nonlinear distortion caused by ultrasonic propagation in living tissue for imaging. In a commercial implement, the second harmonic component is generally used since its amplitude is drastically greater than the amplitude of the higher-order harmonic components. The advantages of THI can be summarized as follows: (i) THI has high-resolution characteristics along the range direction compared to fundamental imaging due to the broadband characteristics of the harmonic components, (ii) THI has high-resolution characteristics along the azimuth direction since the nonlinear effect strongly occurs at the center of the transmitted beam with high sound pressure, and (iii) there are almost no artifacts such as multiple reflection and side lobes in THI since the sound pressure of the echo reflected from the scatterer is low and hence the sound pressure of the multiple reflected echo is further low, and the amplitude of the side lobes of harmonics is 60–80 dB smaller than that of the main lobe. On the other hand, in THI the amplitude of the harmonic components is significantly smaller than the amplitude of the fundamental component. In order to solve this problem, we proposed a method based on the Bayesian estimation using the prior information of the second harmonic echoes introduced from fundamental echoes [11].

Applying a PCT to THI is expected to improve the SNR while maintaining high-resolution characteristics, but frequency-dependent attenuation (FDA) must be strongly aware. FDA causes severe distortion of echo signals, when the broadband pulse propagates through the soft tissue in the living body. Since the high-frequency component attenuates more than the low-frequency component, particularly large distortion occurs in harmonic components. **Figure 1** shows the FDA in the time domain and **Figure 2** shows it in the frequency domain. The distortion of the echo caused by FDA makes exact pulse compression impossible, and, hence, image blurring occurs [10]. In order to prevent the SNR degradation and of the range resolution degradation due to the echo distortion caused by FDA, we have proposed an FDA compensation method [12–14]. In the methods, an amplitude-modulated FM chirp pulse is transmitted, the echo for which is distorted by FDA and, as a result, is received as an ideal waveform. The proper amplitude modification (AM) of the transmission is determined using the FDA characteristic measured by transmitting a reference pulse toward a region of interest (ROI) and receiving the corresponding echo. Since the methods proposed [12, 13] have been constructed for fundamental imaging, this study aims to extend them for THI imaging. The method [13] was constructed for
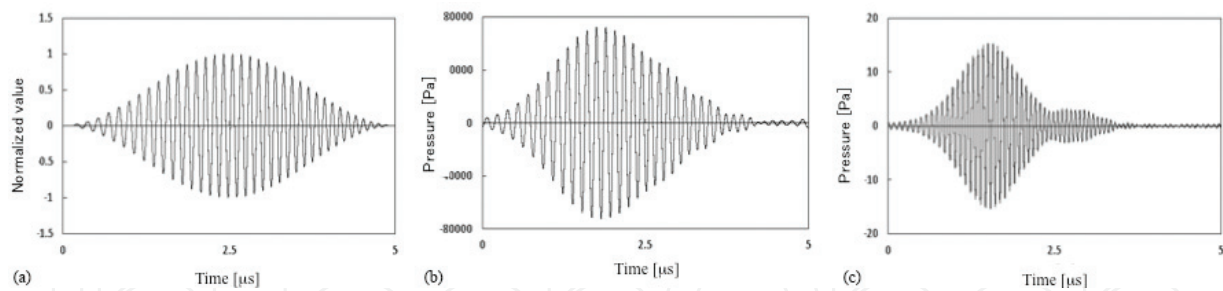
Figure 1. Temporal distortion caused by FDA: (a) transmitted signal, (b) fundamental echo, and (c) second harmonic echo.
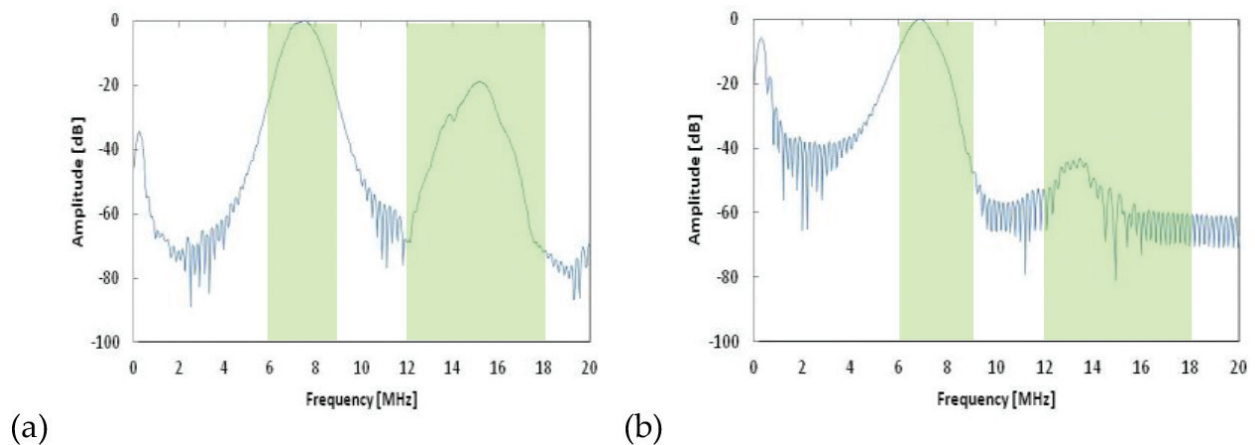

Figure 2. FDA represented in frequency domain: (a) without FDA and (b) after FDA distortion. Green boxes indicate fundamental band and second harmonic band.

harmonic imaging, but the compensation of the transducer characteristics was insufficient, which will be solved in this study to propose an FDA compensation method with high completeness. Typical purposes of AM of an FM chirp signal are side-lobe suppression and compensation of the resonance characteristics of a transducer [15]. The techniques for these purposes can be also integrated into our method. The effectiveness of our method on the harmonic FDA compensation is confirmed through numerical simulations by finite element method (FEM) and simple experiments.

2. Method

2.1. Transducer characteristic compensation

2.1.1. Compensation for fundamental band

Before considering FDA compensation, it is necessary to correct the frequency characteristic of the transducer, which must be done only once for each transducer. For fundamental imaging, the transmission and reception characteristics of the transducer are simply compensated for

both amplitude and phase. To evaluate the characteristic, any arbitrary FM chirp signal $f(t)$ covering the entire frequency band used for imaging is applied as a voltage to the transducer, and the corresponding echo $g(t)$ is received. Their frequency representations are denoted as $F(\omega)$ and $G(\omega)$, respectively. The complex distortion function $R(\omega)$ is defined as follows:

$$R(w) = \frac{H(w)}{G(w)}. \tag{1}$$

In this equation, $H(\omega)$ is the frequency representation of the ideal FM chirp signal and should have spectrum amplitude with a window function suitable for reducing side lobes.

$S(\omega)$ defined by the following equation can be adopted as a transmission pulse for compensating transducer characteristics and observing an appropriate FM chirp echo:

$$S(w) = R(w)F(w). \tag{2}$$

The simulation confirmed that beam focusing has little effect on measuring transducer characteristics.

2.1.2. Compensation for fundamental transmission and harmonic reception

For tissue harmonic imaging, the transmission characteristic in the fundamental frequency band and the reception characteristic in the harmonic frequency band must be corrected at the same time. That is, the harmonic echo is distorted due to the fundamental transmission characteristic and the harmonic reception characteristic. Hereafter, attention is focused only on the second harmonic component. The fundamental transmission characteristic can be evaluated by experimentally measuring the transmitted pressure by a hydrophone. We represent an arbitral FM chirp transmission signal $f_F(t)$ and the corresponding pressure $g_F(t)$ measured in the propagation medium and define the fundamental transmission distortion as $R_F(\omega) = H_F(\omega)/G_F(\omega)$, where $H_F(\omega)$ is a frequency representation of an ideal fundamental FM chirp signal. The harmonic reception distortion is defined as $R_H(\omega) = H_H(\omega)/G_H(\omega)$, where $H_H(\omega)$ is a frequency representation of an ideal second harmonic FM chirp signal. The harmonic reception characteristic can be evaluated by measuring the transmitted pressure $f_H(t)$ and the received echo voltage $g_H(t)$ in the transmission/reception experiment using the frequency band corresponding to the second harmonic frequency under the condition that FDA can be neglected. Furthermore, the mapping from the fundamental component $C_F(\omega)$ to the second harmonic component $C_H(\omega)$ in the frequency domain is defined as follows:

$$C_H(w) = M_{conv}(C_F(w)). \tag{3}$$

In addition, the inverse mapping is also defined as follows:

$$C_F(w) = M_{inv}(C_H(w)). \tag{4}$$

These mapping functions can simply be determined by scaling and shifting the corresponding components on the frequency axis. The scale factor between $C_F(\omega)$ and $C_H(\omega)$ is not important, as it is only intended to reduce the distortion of the spectral shape.

Using these definition and the harmonic pressure $f_H(t)$ generated in the tissue and returned to the transducer, the transmission signal that compensates for the transducer characteristic signal $S_H(\omega)$ can be generated as follows:

$$S_H(w) = R_F(w)M_{inv}(R_H(w)F_H(w)). \tag{5}$$

As the transmitted fundamental pulse propagates toward the ROI, harmonics are gradually generated, and such a detailed process is ignored in the derivation of the above equation. To generate the time signal $s_H(t)$ corresponding to $S_H(\omega)$, it is necessary to perform somewhat complicated experiments. Instead of the experiments, it is realistic to calculate transducer characteristics by simulating exactly the material and structure of the transducer. In this study, we determine the distortion functions $R_F(\omega)$ and $R_H(\omega)$ by simulations. Details of the simulation procedure are described in Section 3. **Figure 3** shows the results of the transducer
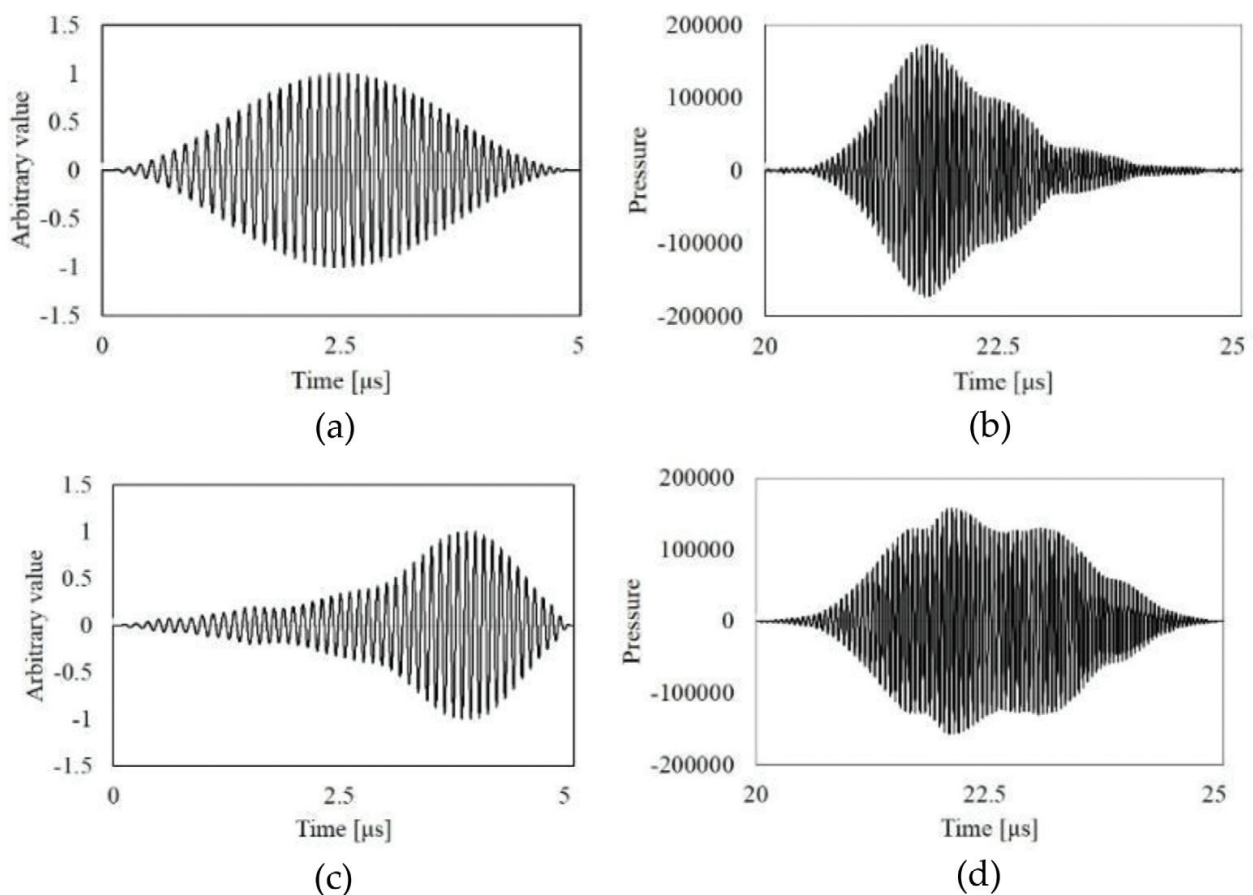

Figure 3. Simulation results of transducer characteristic compensation. Ideal FM chirp signal shown in (a) is applied to transducer, and second harmonic echo in (b) is received without attenuation in water. Signal that compensates for transducer characteristic which is determined by Eq. (5) is shown in (c), and corresponding second harmonic echo is shown in (d).

characteristic compensation. By comparing **Figure 3(b)** and **(d)**, it can be confirmed that the transducer characteristics are almost corrected.

2.2. FDA compensation

2.2.1. Method for fundamental component

FDA compensation can be performed basically in the same way as compensating the characteristics of the transducer. However, it is noted that the FDA compensation should be carried out for each region of interest (ROI) that is required to be finely imaged. To estimate the distortion characteristics caused by FDA in the propagation medium, as a reference transmission for investigation, we transmit $s_F(t)$ defined by Eq. (2) representing a frequency representation, which already compensates for the characteristics of the transducer in the fundamental band, with focusing on the ROI, and we receive the echo signal $e_F(t)$ as voltage. In this study, we assume that the FDA affects the amplitude of the echo signal and that the phase is unaffected. Therefore, the fundamental distortion function of the FDA for the fundamental component $R_{FFDA}(\omega)$ is defined as.

$$R_{FFDA}(w) = \frac{H_F(w)}{E_F(w)}. \tag{6}$$

By using this, the transmission signal $S_{Fcmp}(\omega)$ suitable for compensating the FDA in the fundamental band can be determined as follows:

$$S_{Fcmp}(w) = |R_{FFDA}|S_F(w). \tag{7}$$

The definition of $R_{FFDA}(\omega)$ in Eq. (6) is an ideal formation, and its actual estimate is described in Section 3.4. Therefore, in our previous study [12], the generation of $S_{Fcmp}(\omega)$ is iteratively done, but we confirmed that the FDA can be compensated almost at once [13]. In the following simulations and experiments, the compensation is done with only one reference transmission/reception.

2.2.2. Method for harmonic component

We transmit $s_H(t)$ corresponding to Eq. (5) and receive the corresponding second harmonic echo $e_H(t)$; the second harmonic distortion function of FDA is defined in the same way as in Eq. (6):

$$R_{HFDA}(w) = \frac{H_H(w)}{E_H(w)}. \tag{8}$$

Therefore, the transmission signal $S_{Hcmp}(\omega)$ that compensates for the FDA in the second harmonic band can be determined as follows:

$$S_{Hcmp}(w) = |R_{FFDA}(w)|M_{inv}(|R_{HFDA}(w)|M_{conv}(S_H(w))). \tag{9}$$

It should be noted that the FDA within the fundamental band only occurs in the outbound path from the transducer to the reflective target. However, since the scale factor as a constant

independent of the frequency does not affect the distortion of the waveform, $|R_{FFDA}(\omega)|$ can be used in Eq. (10) without reducing it to half.

The amplitude-modulated FM chirp pulse $s_{Hcmp}(t)$ corresponding to $s_{Hcmp}(\omega)$ is transmitted, and then its echo that is expected to have no FDA distortion is used for imaging. Instead of the proposed modification of the transmission pulse, you can amplify the echo and easily reduce the FDA distortion. However, in this case, the SNR is drastically lowered particularly at the high-frequency portion, and the imaging quality is lowered.

3. Simulations

3.1. Simulation condition for transducer characteristic compensation

The simulations in this study were performed using PZFlex (Weidlinger Associates, Inc.), which is a standard finite element method (FEM) simulator for ultrasound propagation and piezoelectric analysis. A two-dimensional simulation model for determining a transmission signal that compensates transducer characteristics is shown in **Figure 4**. A linear array transducer having 64 oscillating elements of PZT was assumed, and an iron plate was used as a reflector. Parameters of the transmission signal is shown in **Table 1**. To evaluate the characteristics of the transducer purely, FDA should not occur, so the attenuation coefficient of water is set to 0 dB/cm/MHz. The transmission pulse is focused on the front face of the iron plate. The characteristics of the transducer and the signal compensating for it can be confirmed from the simulation results already shown in **Figure 3** in Section 2.1.2.

3.2. Definition of FDA model

In the PZFlex, the definition of FDA is represented as

$$\text{FDA} = d(f_c/f_d)^n \left[\frac{\text{dB}}{\text{cm}}\right], \tag{10}$$

where d is the in vivo attenuation coefficient, f_c is the center frequency, f_d is the measurement frequency, and n is the exponent of FDA. Through the simulations assuming tissue with FDA modeled by logarithmic linear characteristic, namely, $n = 1$, we confirmed that this model is effective [12]. However, a living body generally has logarithmic nonlinear characteristics. Therefore, we experimentally measured the value of n for a phantom mimicking living tissue, and as a result, $n = 1.6$ was obtained, and this value is used in the following simulations.

3.3. Simulation condition for FDA compensation

It is necessary to confirm the effectiveness of our method under medical usage condition assuming a living body. Since it is difficult to verify such effectiveness from the beginning through experiments, two-dimensional FEM simulations were performed using a model shown in **Figure 5** in which the propagation medium imitates the liver and the object corresponds to a tumor. Transmission pulses are formed in the same way as the simulations in
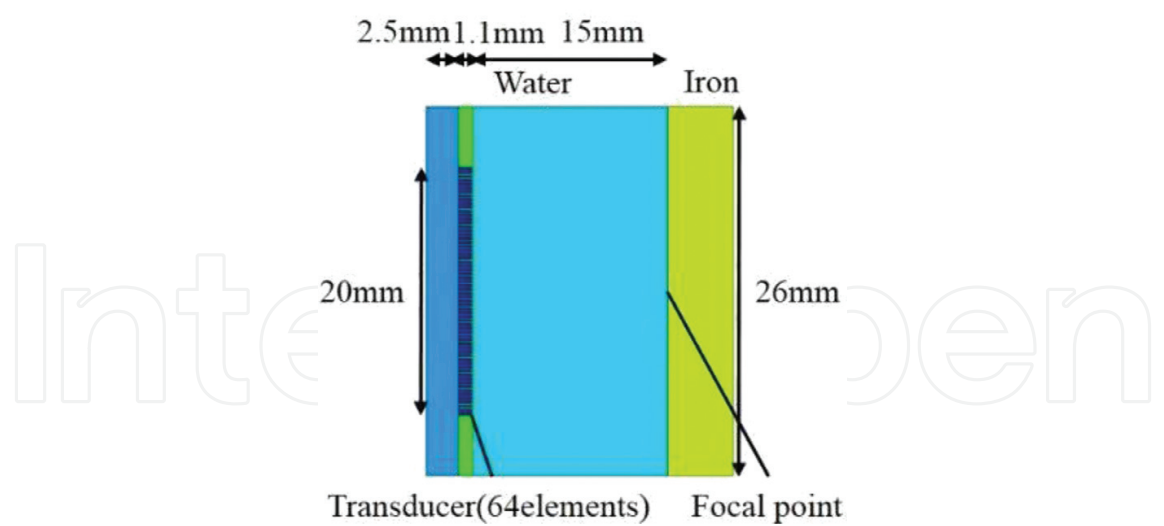
Figure 4. Simulation model for compensating transducer characteristics.

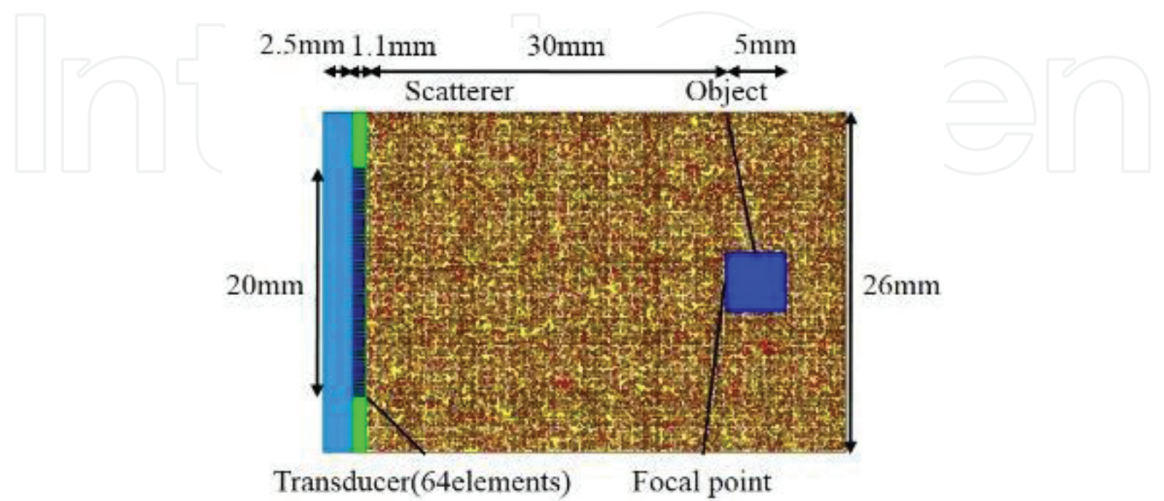| Type of transmission signal	FM chirp with Hanning window
Center frequency [MHz]	10
Frequency bandwidth [MHz]	4
Pulse duration [μm]	5
Focus of transducer [mm]	15
Sampling frequency [MHz]	500
Transmission voltage [V]	40
Number of oscillator elements	64

Table 1. Measurement condition in simulations.

Figure 5. Simulation model for FDA compensation.

Section 3.1 and are focused on 30 mm away from the transducer, i.e., on the front of the target object. Parameters of the transmission signal are also the same as in **Table 1** in Section 3.1. The medium in **Figure 5** consists of scatterers that can mimic the speckle patterns of the liver. Sound speed, density, and attenuation coefficient of each scatterer are randomly defined within the range of **Table 2**. The blue object shown in **Figure 5** mimics the tumor, and its properties are also shown in **Table 2**. We simulate the echoes reflected from the front of the object and analyze them.

3.4. Results of harmonic FDA compensation

The absolute values of R_{FFDA} in Eq. (6) and R_{HFDA} in Eq. (8) must be estimated from the reference echo received by transmitting the FM chirp pulse in Eq. (5) that compensates for the transducer characteristics in order to generate the transmission signal $s_{Hcmp}(t)$ corresponding to Eq. (6), which can compensate for the FDA in the second harmonic band. The dashed line in **Figure 6** is an example of the logarithm of $|R_{FFDA}|$ that was measured by the simulation. From the figure we can know that $|R_{FFDA}|$ is distorted at the high-frequency part and there are several small ripple patterns, which may not be FDA characteristics and may indicate the characteristics of the reflection process and the propagation medium. Therefore, in the actual procedure, the observed $|R_{FFDA}|$ should be approximated by function fitting as a smooth function $|R_{FFDA}|^*$. **Figure 6(a)** shows a linear approximation by line fitting of the log of $|R_{FFDA}|$, and **Figure 6(b)** shows a nonlinear approximation by fifth-order polynomial curve fitting. In actual use, the optimal order of the polynomial function should be determined using appropriate criteria, but in the following

Medium	Sound speed [m/s]	Density [kg/m³]	Attenuation coefficient [dB/cm/MHz]	Nonlinear parameter [B/A]
Liver	1560–1590	1050–1070	0.75–0.95	6.75
Tumor	1900	2500	0.6	7.00

Table 2. Various parameters in simulation model mimicking the liver and tumor.
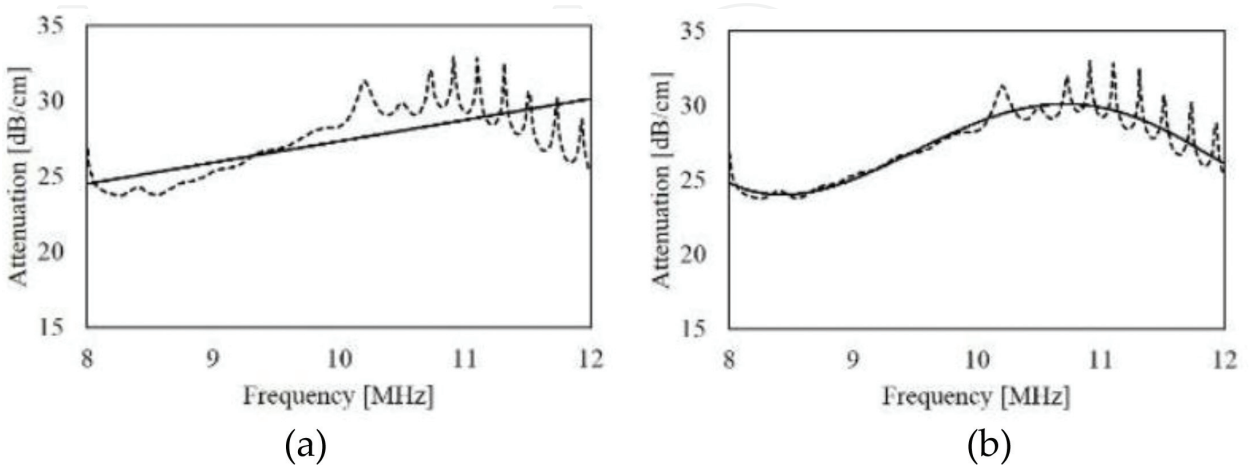

(a)   (b)

Figure 6. Logarithm of $|R_{FFDA}|$ measured by simulations (dashed line) and its approximations $|R_{FFDA}|^*$ with (a) line fitting and with (b) fifth-order polynomial function fitting (solid line).
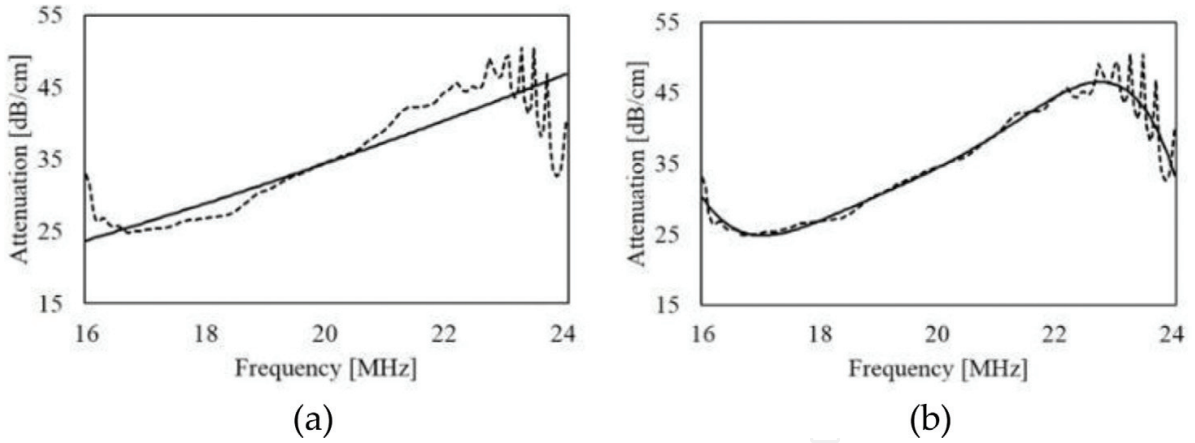
Figure 7. Logarithm of $|R_{HFDA}|$ measured by simulations (dashed line) and its approximations $|R_{HFDA}|^*$ with (a) line fitting and with (b) fifth-order polynomial function fitting (solid line).

simulations and experiments, we compare the performance of line fitting and fifth-order polynomial function fitting. Similarly, the results of R_{HFDA} are shown in **Figure 7**. Comparing **Figures 6** and **7**, it is obvious that the frequency dependence of FDA is larger in the second harmonic band than in the fundamental band, which means that the distortion of the pulse compression echo is large in the second harmonic band, and hence the influence of FDA is very serious for harmonic imaging compared to fundamental imaging.

Figure 8(a) shows the second harmonic component of the echo from the object in **Figure 5** without FDA compensation, i.e., the echo corresponds to $s_H(t)$ which compensates only the transducer characteristics. The spectrum amplitude corresponding to **Figure 8(a)** is shown by the solid line in **Figure 8(b)**. It can be seen that the high-frequency band is greatly attenuated. **Figure 9(a)** is a harmonic echo obtained by transmitting $s_{Hcmp}(t)$ corresponding to Eq. (9) using $|R_{FFDA}|^*$ and $|R_{HFDA}|^*$ approximated by line fitting. The spectrum amplitude is shown in **Figure 9(b)**. **Figure 10** shows the results corresponding to the approximation by fifth-order polynomial function fitting of $|R_{FFDA}|^*$ and $|R_{HFDA}|^*$. From **Figures 9** and **10**, it is confirmed
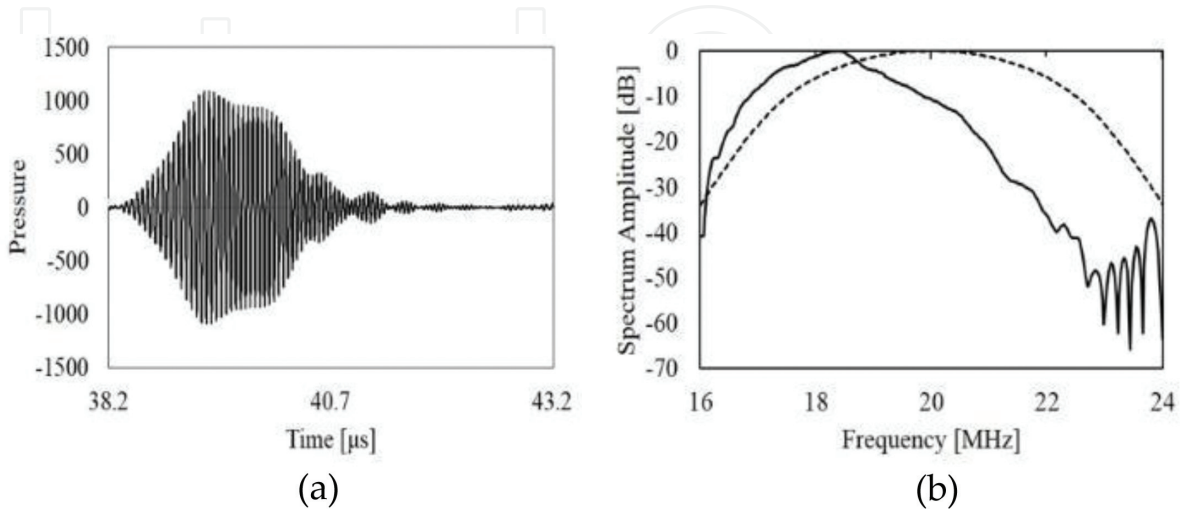

Figure 8. Second harmonic echo obtained by simulation without FDA compensation is shown in (a), and its spectrum amplitude is shown in (b) as solid line with ideal amplitude as dashed line.

that our compensation method based on amplitude-modulated transmission can effectively avoid FDA especially for high-frequency parts. **Figure 11** shows the normalized envelope signals of compressed second harmonic echoes corresponding to **Figures 9(a)** and **10(a)**
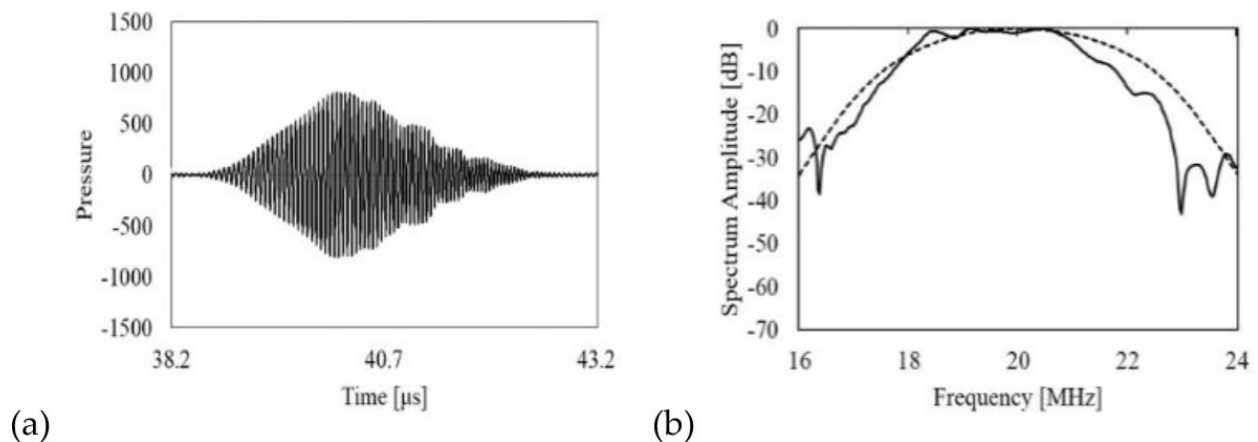

Figure 9. Second harmonic echo obtained by simulation with linear FDA approximation is shown in (a), and its spectrum amplitude is shown in (b) as solid line with ideal amplitude as dashed line.
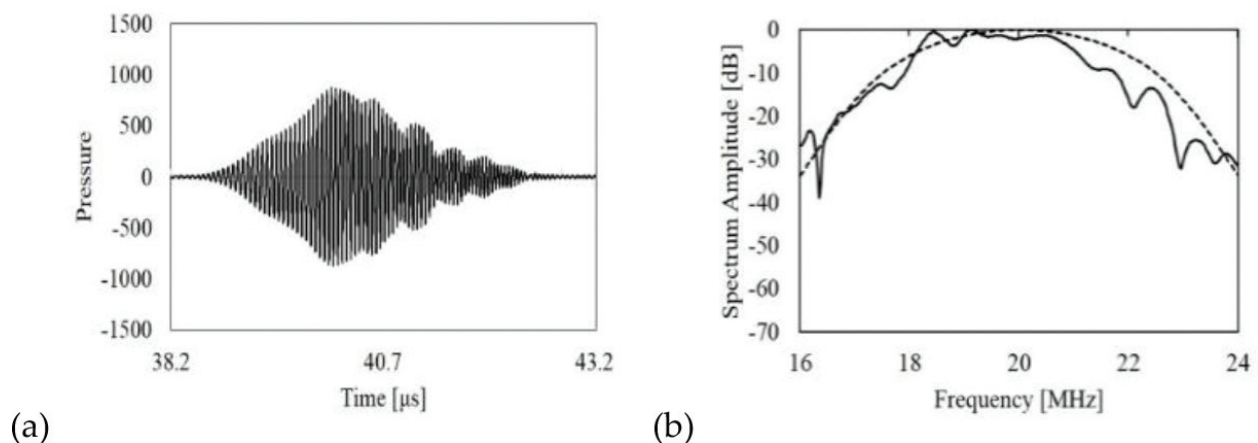

Figure 10. Second harmonic echo obtained by simulation with nonlinear FDA approximation is shown in (a), and its spectrum amplitude is shown in (b) as solid line with ideal amplitude as dashed line.
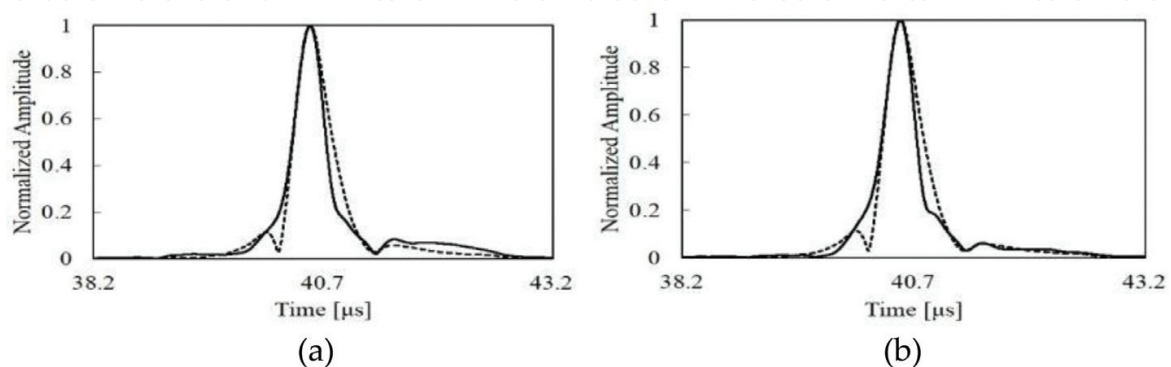

Figure 11. Normalized envelope signal of compressed second harmonic echo obtained by simulation before FDA compensation (dashed line) and after FDA compensation (solid line): (a) with linear FDA approximation and (b) with nonlinear FDA approximation.
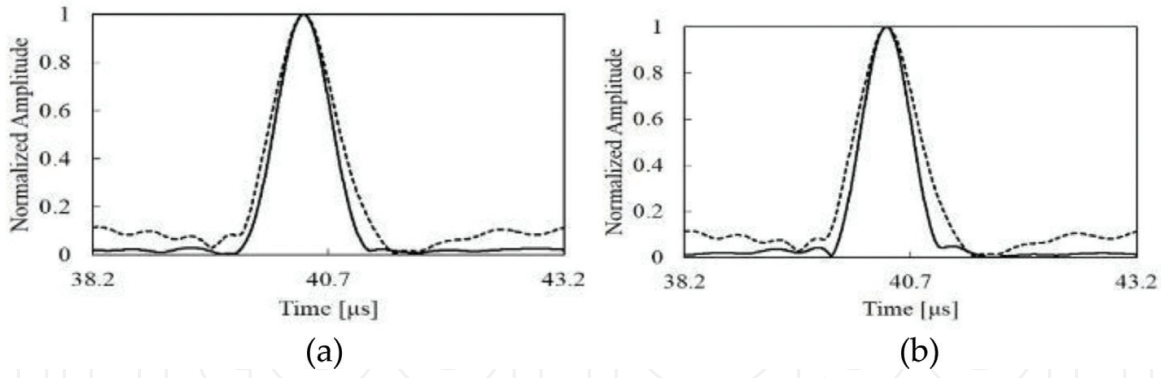
Figure 12. Normalized envelope signal of compressed fundamental echo obtained by simulation before FDA compensation (dashed line) and after FDA compensation (solid line): (a) with linear FDA approximation and (b) with nonlinear FDA approximation.

respectively. The -3 dB pulse width before FDA compensation is 0.442 µs and the -3 dB pulse width after FDA compensation is 0.378 µs with linear approximation and 0.374 µs with nonlinear approximation. The envelope signals of the fundamental echo corresponding to the same transmission of $s_{Hcmp}(t)$ are shown in **Figure 12**. The optimal transmission for compensating FDA in the fundamental band is $s_{Fcmp}(t)$ defined in Eq. (7), but $s_{Hcmp}(t)$ is sufficiently effective against the fundamental FDA compensation.

4. Experiments

4.1. Experimental setup

In order to confirm the actual effectiveness of our FDA compensation, we conducted simple experiments using the experimental system shown in **Figure 13(a)**. The transducer used in the experiments shown in **Figure 13(b)** is SONIX ISI506R having a center frequency of 5 MHz. The amplifier is Amplifier Research 50A15, the function generator is Tektronix APG3102, and the oscilloscope is IWATSU DS-5552. A linear FM chirp signal was transmitted toward the iron
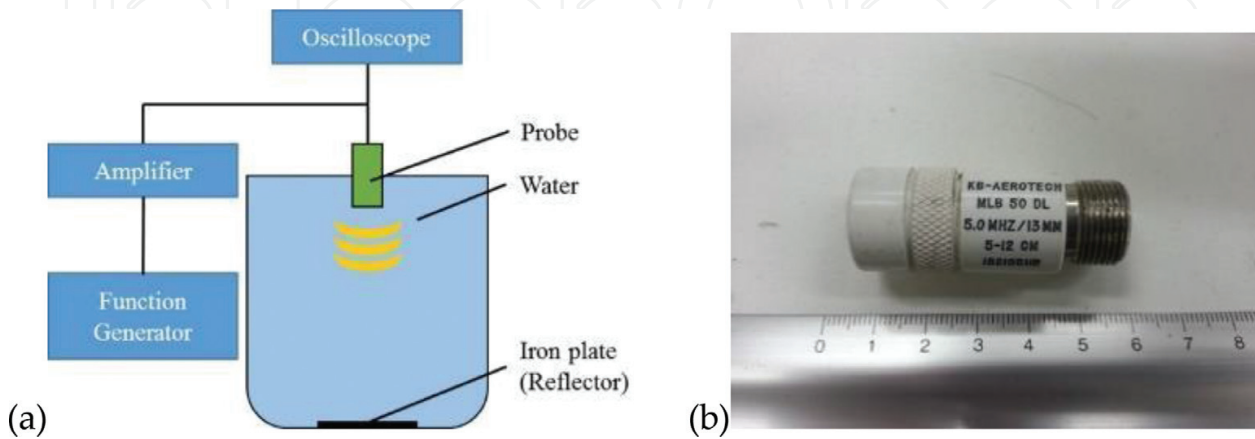

Figure 13. Experimental system is constructed as (a), and (b) indicates probe used in this system.

Type of transmission signal	FM chirp with Hanning window
Center frequency [MHz]	7.5
Frequency bandwidth [MHz]	3
Pulse duration [μm]	10
Focus of transducer [mm]	15
Sampling frequency [MHz]	500
Transmission voltage [V]	40

Table 3. Measurement condition in experiments.

plate placed 15 cm away from the transducer, and the echo reflected from the iron plate was observed. The measurement conditions are shown in **Table 3**. Experimental verification of the characteristics of the transducer can be realized by measurement of transmitted sound pressure in water by a hydrophone. In this issue, we focused on confirming the effect of FDA compensation and conducted experiments using frequency bands with relatively flat transducer characteristics. Hence, in the experiments, the characteristics of the transducer were not taken into account, and only the FDA of water was compensated. That is, instead of $S_H(\omega)$ in Eq. (10), an ideal FM chirp was used to generate a signal to be transmitted.

4.2. Experimental results

In this section, the experimental results of our method for compensating FDA in the second harmonic band caused by water corresponding to a sufficient propagating distance are shown. **Figure 14(a)** shows the experimentally measured echo reflected from the iron plate without FDA compensation. **Figure 14(b)** shows the second harmonic echo extracted from the whole echo of **Figure 14(a)**, and its spectrum amplitude is shown in **Figure 14(c)**. In the high-frequency part in **Figure 14(c)**, the FDA of the second harmonic component is seen. By transmitting a reference signal and estimating $|R_{FFDA}|^*$ and $|R_{HFDA}|^*$ using nonlinear polynomial function fitting, the FDA in the second harmonic band can be compensated. **Figure 15(a)** shows the entire echo with FDA compensation, and the harmonic component and its spectrum amplitude are shown in **Figure 15(b)** and **(c)**, respectively. By comparing **Figures 14(c)** and **15(c)**, the FDA compensation at the high-frequency part can be confirmed, although the FDA is not so large in this experiment. The reason why the FDA is smaller in the experiment than in the simulation
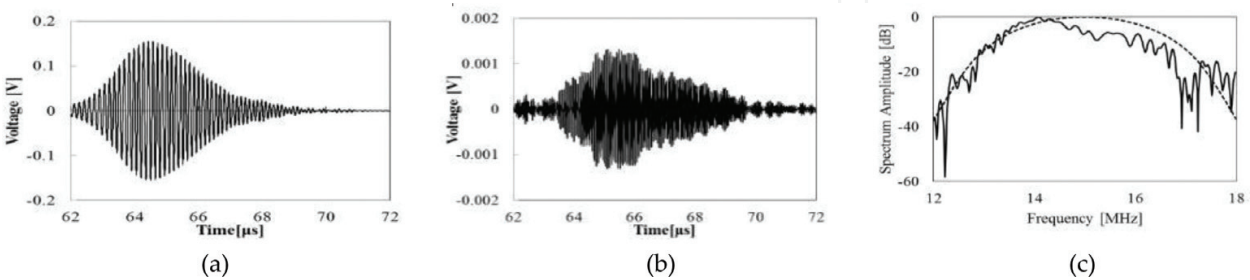

(a)	(b)	(c)

Figure 14. Experimentally received echo without FDA compensation: (a) whole echo, (b) harmonic echo extracted from (a), and (c) spectrum amplitude shown as solid line (ideal amplitude is indicated as dashed line).

Figure 15. Experimentally received echo with FDA compensation using nonlinear approximation: (a) whole echo, (b) harmonic echo extracted from (a), and (c) spectrum amplitude shown as solid line (ideal amplitude is indicated as dashed line).
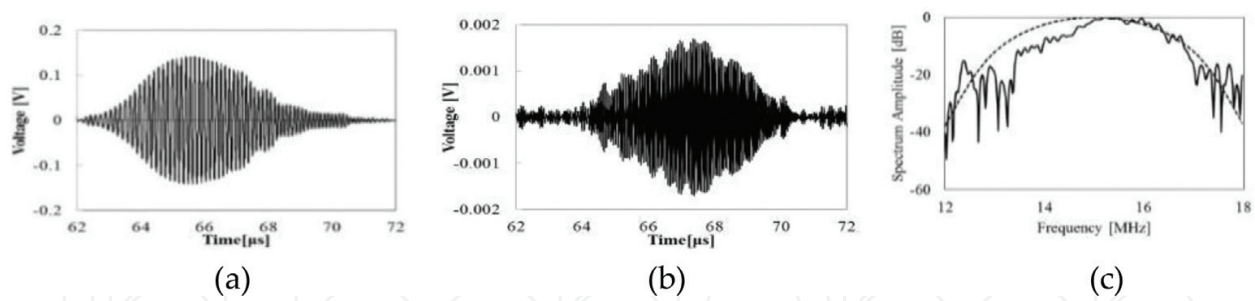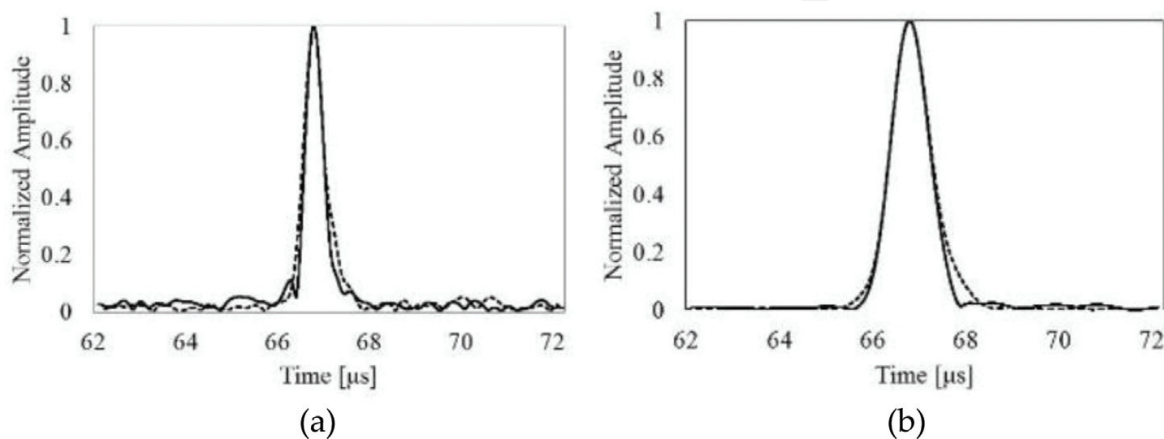

Figure 16. Experimentally obtained envelope signal of compressed echo before FDA compensation (dashed line) and after FDA compensation (solid line): (a) second harmonic one and (b) fundamental one.

is that the water attenuation is considered to be smaller than that in the living body. Therefore, in the future study, we need to use a more attenuated propagation medium that imitates living tissue for experiments. **Figure 16** shows the normalized envelopes of the compressed echo signals before and after FDA compensation. In addition to the second harmonic component in **Figure 16(a)**, the fundamental one is also shown in **Figure 16(b)**. For both the second harmonic component and the fundamental component, the FDA compensation is actually effective.

5. Conclusions

In this study, we proposed a novel and simple method for FDA compensation to realize the fine THI, which can also compensate transducer characteristics. Its effectiveness was confirmed by two-dimensional simulations using a model imitating liver and tumor and by simple experiments. Our method is based on FM chirp pulse compression to realize high SNR, and we expect that fine imaging is effectively performed in a local manner by setting a ROI determined by preimaging by conventional B-mode imaging. In this study, investigation of FDA characteristics is assumed to be performed locally by transmitting a reference signal

and receiving its echo position to be finely imaged. However, it can be considered that such FDA characteristics are invariant in the tissue region having uniform characteristics. This indicates that it is possible to reduce the number of transmission and reception for reference and it becomes easy to obtain the whole high-definition imaging. In the future, we will examine such an extended method and conduct the experiments using a phantom that imitates a living body and also the experiments on living tissue.

In the research field of ultrasound harmonic imaging, mainly the method of extracting the harmonic component appropriately from the echo [16] and the technique to increase the noise resistance of the harmonic component [11] are extensively examined. As sound pressure is higher, large harmonic components are generated, so sharp transmission pulses are generally used in many studies in general. In our study, from the viewpoint of using more energy, we aim to improve the SNR of the harmonic components by using FM chirp pulses, and FDA compensation is important for PCT in order to avoid deterioration of the waveform after compression processing. We are studying a method to enable super resolution by multiple transmission and reception with different carrier frequencies [17], and FDA compensation is also important for applying this method to harmonic components.

Acknowledgements

Author details

Norio Tagawa[1]*, Takuya Hiraoka[1] and Iwaki Akiyama[2]

*Address all correspondence to: tagawa@tmu.ac.jp

1 Faculty of Systems Design, Tokyo Metropolitan University, Tokyo, Japan

2 Doshisha University, Kyoto, Japan

References

[1] Irie T, Hasegawa T, Sato M, Tagawa N, Tanabe M, Yoshizawa M, Iijima T, Moriya T, Itoh K. Transmission of 100-MHz-range ultrasound through a fused quartz fiber. In: Proceeding of IEEE Int. Ultrasonics Symp. 2012. pp. 358-361

[2] Irie T, Hasegawa T, Itoh K, Hirota N, Tagawa N, Yoshizawa M, Moriya T, Iijima T. Tissue imaging using the transmission of 100-Mhz-range ultrasound through a fused quartz fiber. In: Proceeding of IEEE Int. Ultrasonics Symp. 2013. pp. 2010-2013

[3] Irie T, Tagawa N, Yoshizawa M, Moriya T. A study for B-mode imaging using 100-MHz-range ultrasound through a fused quartz fiber. In: Proceeding of IEEE Int. Ultrasonics Symp., CD. 2015

[4] Chiao RY, Hao X. Coded excitation for diagnostic ultrasound: A system developer's perspective. IEEE Transactions on Ultrasonics, Ferroelectrics, and Frequency Control. 2005;**52**:160-170

[5] Hu Z, Moriya T, Tanahashi Y. Imaging system for intravascular ultrasonography using pulse compression technique. Japanese Journal of Applied Physics. 2001;**40**:3896-3899

[6] Misaridis T, Jensen JA. Use of modulated excitation signals in medical ultrasound. IEEE Transactions on Ultrasonics, Ferroelectrics, and Frequency Control. 2005;**52**:177-192

[7] Akiyama I, Yoshizumi N, Saito S, Wada Y, Koyama D, Nakamura K. Development of multiple-frequency ultrasonic imaging system using multiple resonance piezoelectric transducer. Japanese Journal of Applied Physics. 2012;**51**:07GF02-1-07GF02-9

[8] Ishiguro Y, Zhu J, Okubo T, Tagawa N, Okubo K. Piezoelectric characteristic analysis of diaphragm type PZT oscillator. In: Proceeding of IEEE Int. Ultrasonics Symp. CD. 2016

[9] Frijlink ME, Goertz DE, van Damme CA, Krams R, van der Steen AFW. Intravascular ultrasound tissue harmonic imaging in vivo. IEEE Transactions on Ultrasonics, Ferroelectrics, and Frequency Control. 2006;**53**:1844-1852

[10] Szabo TL. Diagnostic Ultrasound Imaging: Inside Out, Chap. 4. Elsevier; 2004

[11] Yamamura T, Tanabe M, Okubo K, Tagawa N. A method for improving signal-to-noise ratio of tissue harmonic imaging based on Bayesian inference using information of fundamental echoes. Japanese Journal of Applied Physics. 2012;**51**:07GF01-1-07GF01-12

[12] Koumoto K, Tagawa N, Okubo K, Akiyama I. Wide band pulse compression imaging with transmission compensation for frequency dependent attenuation In: Proceeding of IEEE Int. Ultrasonics Symp 2012. pp. 1658-1661

[13] Hiraoka T, Tagawa N, Okubo K, Akiyama I. Recursive reduction of frequency dependent attenuation for wide-band ultrasound imaging in a living body. In: Proceeding of IEEE Int. Ultrasonics Symp. 2013. pp. 914-917

[14] Hiraoka T, Tagawa N, Okubo K, Akiyama I. Compensation method of frequency dependent attenuation for tissue harmonic imaging. In: Proceeding of IEEE Int. Ultrasonics Symp., CD. 2014

[15] Levanon N, Mozeson E. Radar Signals. Wiley Inter-science; 2004

[16] Hasegawa H, Tanaka H, Takezaki T, Machida S. Amplitude modulated pulse inversion technique for high SNR of tissue harmonic imaging using CMUT. In: Proceeding of IEEE Int. Ultrasonics Symp. CD. 2017

[17] Wada T, Ho Y, Okubo K, Tagawa N, Hirose Y. High frame rate super resolution imaging based on ultrasound synthetic aperture scheme. Physics Procedia. 2015;**70**:1216-1220